Available online at www.sciencedirect.com
SCIENCE DIRECT®
Journal of Molecular Catalysis A: Chemical 225 (2005) 47–58
JOURNAL OF MOLECULAR CATALYSIS A: CHEMICAL
www.elsevier.com/locate/molcata

Influence of the ion exchanged metal (Cu, Co, Ni and Mn) on the selective catalytic reduction of NO_X over mordenite and ZSM-5

A. De Lucas, J.L. Valverde, F. Dorado, A. Romero, I. Asencio*

Departamento de Ingeniería Química, Facultad de Ciencias Químicas, Universidad de Castilla-La Mancha, 13004 Ciudad Real, Spain

Received 7 June 2004; accepted 1 August 2004
Available online 2 October 2004

Abstract

Selective catalytic reduction of NO by propene was investigated on Cu, Co, Ni and Mn ion-exchanged ZSM-5 and mordenite in the presence of excess of oxygen. The properties of the catalysts were studied by X-ray diffraction, temperature-programmed desorption/reduction and atomic absorption. H_2-TPR results showed that for copper catalysts metal was mainly present in the form of isolated Cu^{2+} strongly coordinated to the framework oxygen atoms of the zeolite. Cobalt, nickel and manganese were present in the form Co^{2+} and Co^{3+}, Ni^{2+}, Mn^{3+} and Mn^{4+}, respectively. The catalytic activity showed for all the catalysts increased with increasing metal content reaching a maximum of NO_X conversion, and then decreased at higher contents. In turn, NO_X conversion increased with the reaction temperature passing through a maximum, and then decreased at higher temperatures, due to the combustion of the hydrocarbon. NO TOF for all the catalysts here prepared was analyzed at 375–425 °C. It was observed that this parameter decreased abruptly with the metal content and, regardless the type of zeolite and ion exchanged metal introduced in the catalysts, all the experimental points were well correlated by an unique curve.
© 2004 Elsevier B.V. All rights reserved.

Keywords: Selective catalytic reduction; Nitrogen oxides; Mordenite; ZSM-5

1. Introduction

Much research related to the selective catalytic reduction of NO_X by hydrocarbons was undertaken and reported in the literature due to its potential for the effective control of NO emission in oxidant environment [1–12]. This reaction has been described as a method to remove NO_X from natural-gas-fueled engines, such as lean-burn gas engines in cogeneration systems [13] and lean-burn gasoline and diesel engines where the noble-metal three ways catalysts are not effective in the presence of excess oxygen [14]. Hydrocarbons would be the preferred reducing agents over NH_3 because of the practical problems associated with its use: handling and slippage through the reactor.

In 1986, Iwamoto et al. [15] reported the activity of Cu-ZSM-5 for the catalytic decomposition of NO_X. Following this finding, many catalysts such as V_2O_5–WO_3 (or MoO_3)/TiO_2, other transitions metal oxides (e.g. Fe, Cr, Co, Ni, Cu, Nb, etc.) and doped catalysts, as well as zeolite-type catalysts have been found active in this reaction.

Earlier studies were mainly focused on the developing catalysts with ZSM-5 as the porous support [16–20]. Shimizu et al. [19,20] recently reported that Cu-aluminate catalysts, containing highly dispersed Cu^{2+} ions in the aluminate phase, showed high de-NO_X activity comparable to the Cu-ZSM-5 and higher hydrothermal stability. On the other hand, Cu ion exchanged Ti-PILCs demonstrated the best performance when using ethylene and propylene as reductants [14,21].

Recently, we have reported several works based on the use of Ti-PILC-based catalysts for the selective catalytic reduction of NO_X using propylene as the reducing agent [21–24]. It was demonstrated that Ti-PILCs ion exchanged with Cu were the most effective catalysts for SCR of NO_X, as compared as those ion exchanged with Ni and Fe. Likewise, it was observed that the presence of 10% water in the feed inhibited the activity of the catalysts. However, the addition of ceria as a cocation to Cu-Ti-PILC catalysts lightly de-

* Corresponding author. Tel.: +34 926295300; fax: +34 926295318.
E-mail address: isaac.asencio@uclm.es (I. Asencio).

1381-1169/$ – see front matter © 2004 Elsevier B.V. All rights reserved.
doi:10.1016/j.molcata.2004.08.036

creased the reversible inhibition by water occurring under reaction conditions. A similar conclusion was reported using Co-exchanged mordenite catalysts [25]. Finally, it was possible to partly prevent the catalyst deactivation and decrease the inhibiting water and sulphur effect by addition of silver as a cocation to these catalysts.

Despite of the large number of references in literature, few extensive studies dealing to the comparison of the catalytic activity for the SCR of NO_X of different catalysts have been reported. In one of these studies we compared the catalytic performance of Cu-ZSM-5-based and Cu-Ti-PILC-based catalysts [26]. The latter were reported to be more active than the former because the redox cycle occurred more easily on the pillared catalysts.

In this work the parent ZSM-5 was in the sodium form. According to Torre-Abreu et al. [27], Cu-mordenite catalysts prepared from the sodium form exhibited much higher activity than those prepared from the acid form. Their results showed that Brönsted acidity does not promote the NO selective reduction by propene. On the other hand, Bulanek et al. [28] observed that the copper present in zeolite together with a sodium cation was easier reduced than in CuH-zeolites.

The aims of this work are:

(a) Comparing the catalytic reduction of NO by propene on both Na-ZSM-5-based and Na-Mordenite-based catalysts ion exchanged by Cu, Co, Ni and Mn.
(b) Characterizing all the catalysts here prepared in order to relate physical and chemical properties to the catalytic behaviour of the two sets of catalysts.

2. Experimental

2.1. Catalysts preparation

Zeolite mordenite was supplied in the sodium form by PQ Corp. with an atomic ratio Si/Al = 7.5 and crystallinity = 100%. Na-ZSM-5 zeolite (Si/Al ratio of 20) was synthesized according to the method described elsewhere [29,30] using ethanol as the template. X-Ray diffraction (XRD) confirmed that the product was 100% crystalline. Metal was introduced by conventional ion exchange using 25 mL of 0.1 M metal aqueous solution per gram of zeolite.

The next compounds were used: $Cu(CH_3COO)_2{\cdot}H_2O$, $Co(CH_3COO)_2{\cdot}4H_2O$, $Ni(NO_3)_2{\cdot}6H_2O$ and $Mn(CH_3COO)_2{\cdot}4H_2O$. The mixture was kept under agitation at the desired temperature (30, 55 or 80 °C) for 14 h. Next, the suspension was filtered and thoroughly washed with deionized water in order to completely remove the occluded salt, and the solid was then air dried at 120 °C for 14 h. The whole procedure was repeated twice for some catalysts. Finally, the samples were air-calcined at 550 °C for 4 h. Table 1 summarizes the catalysts here prepared. These catalysts were referred to as a function of the temperature of ion exchange and number of ion exchange steps. For instance, Ni-1-55-ZSM-5 corresponds to a nickel-zeolite ZSM-5 exchange once at 55 °C. The ion exchange level included in Table 1 was determined taking as a reference the number of aluminium atoms contained in the structure.

2.2. Catalyst characterization

The X-ray diffraction (XRD) patterns were measured with a Philips model PW 1710 diffractometer with Ni-filtered Cu Kα radiation.

The metallic content (wt.%) of the prepared catalysts was determined by atomic absorption measurements by using a SPECTRAA 220FS analyzer. The samples were previously dissolved in hydrofluoric acid and diluted to the interval of measurement. In all cases, calibrations from the corresponding patron solutions were performed.

Total acid-site density and acid-strength distribution of each of the catalysts were measured by temperature-programmed desorption (TPD) of ammonia, using a Micromeritics TPD/TPR 2900 analyzer. The samples were housed in a quartz tubular reactor and pretreated in a flow of helium while heating at 15 °C/min up to the calcination temperature of the sample. After a period of 30 min at this temperature, the samples were cooled to 180 °C and saturated for 15 min in a stream of ammonia. The catalyst was then allowed to equilibrate in a helium flow at 180 °C for 1 h. The ammonia was then desorbed by using a linear heating rate of 15 °C/min up to 900 °C. Temperature and detector signals were simultaneously recorded. Total acidity is defined as the total acid site density, which is obtained by integration of the area under the curve. To obtain the strength distribution, the desorption profiles were fitted using two peaks, the maximum and width of these peaks being held as constant as possible while fitting each profile. Weak and strong acidities are defined as the concentration of weak and strong acid sites, respectively, obtained by integration of the area under the peaks at the lowest and highest temperatures, respectively. These peaks were not assigned to a specific acid site (Brönsted or Lewis), but it was a convenient way to categorize the acid strength distribution obtained by this method.

TPR measurements were carried out with the same apparatus described above. After loading, the sample was outgassed by heating at 15 °C/min in an argon flow up to the calcination temperature of the sample and kept constant at this temperature for 30 min. Next, it was cooled to room temperature and stabilized under an argon/hydrogen flow (≥99.9990% purity, 83/17 volumetric ratio). The temperature and detector signals were then continuously recorded while heating at 15 °C/min up to 900 °C. The liquids formed during the reduction process were retained by a cooling trap placed between the sample and the detector.

2.3. Catalyst activity measurements

The experiments were carried out at atmospheric pressure in a flow-type apparatus designed for continuous operation.

Table 1
Composition and characterization of zeolite-based catalysts

Catalyst	Sodium content (wt.%)	Ion exchange steps and temperature (°C)	Metal content (wt.%)	Ion exchange level (%)	Weak acid sites density (mmol NH_3/g)	Strong acid sites density (mmol NH_3/g)
Na-MOR	6.1	–	0.0	0	0.624 (290)	Not detected
Cu-1-30-MOR	0.9	1–30	3.2	53	0.619 (291)	0.787 (627)
Cu-1-55-MOR	0.8	1–55	3.5	60	0.642 (284)	0.799 (619)
Cu-1-80-MOR	0.8	1–80	4.8	81	0.657 (282)	1.350 (614)
Cu-2-30-MOR	0.6	2–30	4.6	77	0.922 (302)	1.255 (650)
Cu-2-55-MOR	0.5	2–55	5.0	84	0.851 (307)	1.055 (645)
Cu-2-80-MOR	0.5	2–80	8.6	147	1.306 (320)	0.821 (640)
Co-1-30-MOR	2.8	1–30	3.0	55	0.785 (273)	0.300 (638)
Co-1-55-MOR	2.7	1–55	3.1	56	0.792 (276)	0.289 (639)
Co-1-80-MOR	2.3	1–80	3.2	58	0.782 (280)	0.286 (642)
Co-2-30-MOR	2.3	2–30	3.8	69	0.910 (290)	0.339 (640)
Co-2-55-MOR	2.0	2–55	4.0	73	0.888 (285)	0.316 (641)
Co-2-80-MOR	1.8	2–80	5.0	91	0.817 (294)	0.320 (640)
Ni-1-30-MOR	3.2	1–30	2.4	44	0.842 (274)	0.466 (541)
Ni-1-55-MOR	3.0	1–55	2.5	46	0.825 (284)	0.488 (537)
Ni-1-80-MOR	2.8	1–80	2.7	49	0.807 (284)	0.575 (537)
Ni-2-30-MOR	2.3	2–30	3.0	55	0.809 (283)	0.701 (543)
Ni-2-55-MOR	2.2	2–55	3.2	58	0.746 (279)	0.774 (540)
Ni-2-80-MOR	2.0	2–80	3.3	60	0.737 (285)	0.809 (535)
Mn-1-30-MOR	3.1	1–30	1.8	35	0.767 (284)	0.291 (586)
Mn-1-55-MOR	2.7	1–55	2.2	43	0.687 (270)	0.299 (590)
Mn-1-80-MOR	2.1	1–80	2.8	54	0.674 (275)	0.293 (590)
Mn-2-30-MOR	2.1	2–30	3.0	58	0.741 (284)	0.374 (605)
Mn-2-55-MOR	2.0	2–55	3.2	62	0.683 (292)	0.382 (591)
Mn-2-80-MOR	2.0	2–80	3.7	72	0.674 (301)	0.386 (595)
Na-ZSM-5	3.2	–	0.0	0	0.950 (295)	Not detected
Cu-1-30-ZSM-5	0.2	1–30	2.4	96	0.830 (291)	0.051 (639)
Cu-1-55-ZSM-5	0.2	1–55	2.6	105	0.708 (295)	0.114 (640)
Cu-1-80-ZSM-5	0.1	1–80	4.4	179	0.531 (310)	0.209 (640)
Cu-2-30-ZSM-5	0.1	2–30	2.9	119	0.782 (282)	0.125 (641)
Cu-2-55-ZSM-5	0.1	2–55	3.7	151	0.658 (303)	0.123 (640)
Cu-2-80-ZSM-5	0.1	2–80	14.3	600	0.675 (312)	0.252 (642)
Co-1-30-ZSM-5	2.8	1–30	0.5	22	0.532 (290)	0.038 (550)
Co-1-55-ZSM-5	2.3	1–55	0.9	39	0.568 (292)	0.065 (551)
Co-1-80-ZSM-5	1.7	1–80	2.2	96	0.539 (290)	0.174 (549)
Co-2-30-ZSM-5	2.5	2–30	0.8	35	0.504 (294)	0.054 (550)
Co-2-55-ZSM-5	2.1	2–55	1.6	70	0.409 (295)	0.131 (552)
Co-2-80-ZSM-5	1.7	2–80	3.1	136	0.332 (290)	0.189 (550)
Ni-1-30-ZSM-5	1.9	1–30	0.3	13	0.533 (301)	0.070 (530)
Ni-1-55-ZSM-5	1.7	1–55	0.6	26	0.439 (298)	0.107 (529)
Ni-1-80-ZSM-5	1.6	1–80	0.8	35	0.421 (294)	0.145 (532)
Ni-2-30-ZSM-5	1.8	2–30	0.5	22	0.455 (290)	0.073 (530)
Ni-2-55-ZSM-5	1.6	2–55	0.7	31	0.447 (291)	0.118 (530)
Ni-2-80-ZSM-5	1.2	2–80	1.1	48	0.405 (296)	0.192 (533)
Mn-1-30-ZSM-5	2.0	1–30	0.3	14	0.465 (300)	0.056 (616)
Mn-1-55-ZSM-5	1.8	1–55	0.7	33	0.441 (293)	0.067 (516)
Mn-1-80-ZSM-5	1.6	1–80	1.2	56	0.382 (293)	0.070 (525)
Mn-2-30-ZSM-5	1.9	2–30	0.7	33	0.444 (290)	0.061 (525)
Mn-2-55-ZSM-5	1.6	2–55	1.0	47	0.431 (293)	0.070 (528)
Mn-2-80-ZSM-5	1.4	2–80	1.8	84	0.372 (296)	0.075 (536)

Temperatures corresponding to the maximum of the desorption peak are included in parenthesis together with the acid sites density value (°C).

This set-up consisted of a gas feed system for each component with individual control by mass flow meters, a fixed-bed down flow reactor and an exit gas flow meter. The reactor, a stainless steel tube with an internal diameter of 4 mm, was filled with the catalyst sample (0.25 g). A temperature programmer was used with a K-type thermocouple installed in contact with the catalyst bed. The products were analyzed simultaneously by chemiluminiscence (NO-NO_2-NO_X ECO PHYSICS analyzer) and by a FT-IR analyzer (PERKIN ELMER Spectrum GX) capable of measuring continuously and simultaneously the following species: NO, NO_2, N_2O, CO_2 and C_3H_8.

The catalysts were brought to identical reaction conditions for each test (1000 ppm C_3H_6, 1000 ppm NO, 5% O_2, and the balance He; space velocity (GHSV) of 15,000 h^{-1} and a flow rate of 125 ml/min). Before the reaction was started, the catalysts were preconditioned at 550 °C for 60 min by flowing helium over the sample (125 ml/min). After this, the temperature was down to 200 °C. The feeding gases were mixed and preheated prior to entering the reactor.

The reaction products were analyzed after 30, 60, 90 and 120 min from the beginning of the experiment. Conversion of NO_X to N_2 shown in all tables is the arithmetic mean of these four analyses, the differences between them being always less than 2%.

3. Results and discussion

3.1. Cu-zeolite-based catalysts

Table 1 lists, for all the catalysts, the sodium and ion exchanged metal content, the ion exchange level and both the weak and strong acid sites density.

It can be observed that, except for the Cu-1-30-ZSM-5, all the ZSM-5-based catalysts presented more Cu content than that corresponding to 100% ion exchange. In turn, only the mordenite-based catalysts with the highest Cu content (Cu-2-80-MOR) presented an ion exchange level higher than this value. Likewise it is also noted for both set of catalysts that for the same number of ion exchange steps, the copper loading increased with increasing ion exchange temperature. An identical effect is observed when, for the same temperature, the number of ion exchange steps increases.

All the catalysts contained sodium ions. As expected, the loading of these ions decreased with increasing copper content. Anyway, it is clear that acidity is a combination of two effects: the presence of Cu and Na on the catalysts.

According to Sachtler and Zhang [31], the first Cu ions would occupy the hidden positions, located in the small cages of the zeolites. Whereas in zeolite Y these hidden positions are located in the sodalite cages, in ZSM-5 these positions appear in the five members units, located in the main framework of channels. In mordenite, these positions are also located in the main framework of channels.

The copper species located in these hidden positions are not easily accessible for ammonia molecules. Since multiple ion exchange steps are needed to achieve the complete filling of small cages, the increase of copper content would lead copper species to be incorporated at more accessible positions. As a consequence the acidity increases.

All the catalysts showed strong acid sites. Mordenite-based catalysts showed, even for similar metal contents, higher density of acid sites than ZSM-5-based ones. This fact is due, not only to the presence of Lewis acid sites on the zeolite but also to the possible ammonia reduction of some cations Cu^{2+}, yielding Brönsted acid sites on the zeolite [31].

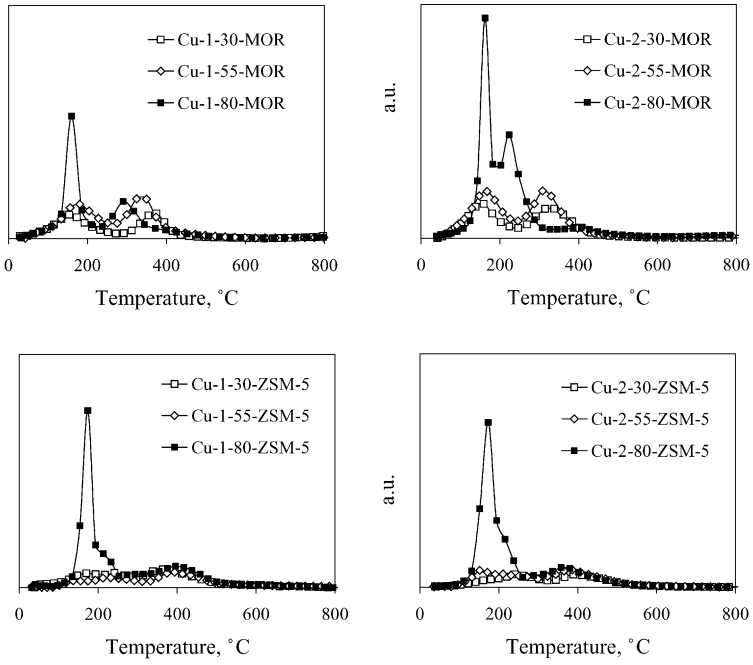

Fig. 1. TPR profile of the copper mordenite-based catalysts.

Fig. 1 presents TPR profile for the catalysts prepared with different Cu contents. According to Delahay et al. [32], the reactions involved in the copper reduction process are:

$$CuO + H_2 \rightarrow Cu^0 + H_2O$$

$$Cu^{2+} + 0.5H_2 \rightarrow Cu^+ + H^+$$

$$Cu^+ + 0.5H_2 \rightarrow Cu^0 + H^+$$

At lower metal contents, the main specie over the catalysts is Cu^{2+}, which can be reduced in two steps to Cu^0. The reduction $Cu^{2+} \rightarrow Cu^+$ occurs at lower temperatures, while the reduction $Cu^+ \rightarrow Cu^0$ would occur at higher temperatures [28,33,34]. When the copper content in the sample is higher, the excess copper may be found as oxygenated clusters easier to reduce than the isolated copper species [14,28,35,36].

All the copper exchanged catalysts show TPR profiles with two reduction peaks, suggesting a reduction process of the isolated Cu^{2+} in two steps. The low temperature peak would indicate the process $Cu^{2+} \rightarrow Cu^+$. The second peak, at higher temperature, would correspond to the process of $Cu^+ \rightarrow Cu^0$.

In the case of ZSM-5-based catalysts, a peak appeared to 180 °C, more intense in the samples ion exchanged at 80 °C (with higher metal content). This peak would be related to the presence of aggregates of CuO. The sample Cu-2-80-MOR also showed this peak. The rest of the mordenite-based catalysts did not show this peak, due probably to the copper content did not exceed the entire ion exchange capacity of this zeolite.

Anyway, the absence of the line of the diffraction of CuO species in the XRD analysis would demonstrate these particles to have a size lower than 3 nm [32], thus justifying the difference of reduction temperature maximum for both zeolites. The presence of these particles of CuO could also be related, according to the acidity measurements, to the occurrence of strong acid sites.

On the other hand, a shift of the second peak ($Cu^+ \rightarrow Cu^0$) to lower temperatures occurs with increasing metal contents, indicating that Cu^+ species would be more difficult to reduce with decreasing copper content. In the case of the ZSM-5 catalysts ion exchanged at 80 °C, an overlap of the peaks corresponding to the reductions $CuO \rightarrow Cu^0$ and $Cu^{2+} \rightarrow Cu^+$ was observed due to their high metal contents.

Fig. 2 shows, for all copper catalysts, the entire consumption of H_2 (mol H_2/mol Cu), in the TPR experiments. In all samples, this consumption was lower than the unit. This fact would indicate that the Cu species present in both types of zeolites are difficult to reduce to a lower valence. Again, the presence of metal ions in hidden positions, not easy to access and difficult to reduce (high activation energy for the reduction process [31]) could explain this behaviour. In these positions, Cu^{2+} species would be strongly coordinated with the framework oxygen atoms of the zeolite.

On the other hand, the entire consumption of H_2 decreases in ZSM-5-based catalysts with increasing metal contents, whereas in the case of mordenite-based catalysts this consumption increases after passing through a minimum. These differences of behaviour could be explained attending to the higher ion exchange capacity and pore size of mordenite.

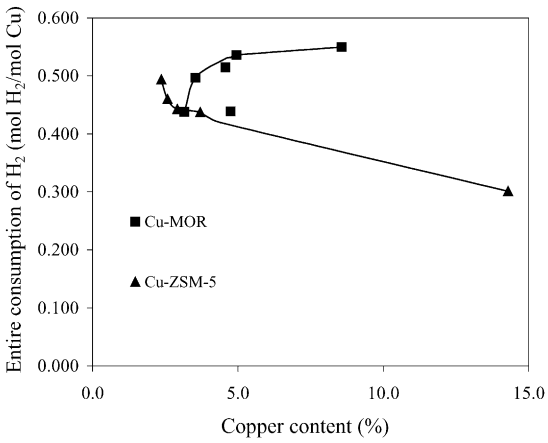

Fig. 2. Entire consumption of H_2 for copper catalysts.

3.1.1. Catalytic activity

Several authors have shown the influence of the copper content in the catalytic activity of different kinds of catalysts for the SCR of NO_X using hydrocarbons as reduction agents. Iwamoto et al. [37] noted that the activity of Cu-ZSM-5 increased with the copper content reaching a maximum for an ion exchange degree between 80 and 100%. On the other hand, Corma et al. [38] showed, in copper ion exchanged-Beta zeolite, that the most active catalysts were the over-exchanged catalyst (with a metal content over the ion exchange zeolite capacity). Torre-Abreu et al. [27] reported different results depending on the ion initially present on the zeolite. When sodium form was used as the basis for the ion exchange, the catalyst obtained had better activity for the catalytic reduction of NO_X. These results would indicate that Brönsted acid sites are not suitable for SCR of NO_X. Bulanek et al. [28] confirmed these results and showed that sodium zeolites were easier to reduce than hydrogen zeolites. These conclusions would justify the use of sodium zeolite as the parent materials.

Table 2 shows, for all catalysts here prepared, the NO_X conversion to N_2 versus the reaction temperature. Maximum values of NO_X conversion for each of catalysts are indicated in bold. It can be observed that the presence of copper can improve the catalytic activity.

With an increase in the reaction temperature, the NO_X conversion increased passing through a maximum, and then decreased at higher temperatures. According to Yang et al. [14], the decrease of this NO_X conversion at higher temperatures was due to the combustion of the hydrocarbon, which reduced the amount of reductant. As seen in Table 2, all the catalysts show a maximum of the conversion of NO_X to N_2 in the range 350–425 °C.

Likewise, the catalytic activity increased with the Cu loading reaching a maximum of NO_X conversion, and then de-

Table 2
NO_X conversion to N_2 for the Cu-zeolite-based catalysts (no N_2O detected)

Catalyst	W_{Cu} (wt.%)[a]	T_u (°C)[b]	NO_X conversion to N_2 (%)									
			T_R[c] = 200 °C	T_R = 250 °C	T_R = 300 °C	T_R = 325 °C	T_R = 350 °C	T_R = 375 °C	T_R = 400 °C	T_R = 425 °C	T_R = 450 °C	T_R = 475 °C	T_R = 500 °C
Cu-1-30-MOR	3.2	30	9.9	11.0	24.7	53.4	58.9	65.1	**68.1**	64.3	60.4	57.5	54.8
Cu-1-55-MOR	3.5	55	10.9	16.8	35.0	55.1	59.0	63.4	**68.7**	65.8	65.0	62.8	58.9
Cu-1-80-MOR	4.8	80	16.9	24.5	39.7	51.7	55.5	60.2	63.4	68.4	70.7	**74.8**	57.4
Cu-2-30-MOR	4.6	30	11.5	13.7	35.4	51.4	59.2	**62.0**	54.4	48.0	43.9	40.7	35.7
Cu-2-55-MOR	5.0	55	8.1	17.5	31.2	34.0	43.1	53.1	56.9	59.4	**61.3**	56.9	53.1
Cu-2-80-MOR	8.6	80	14.9	14.6	21.9	28.9	36.3	42.6	44.7	**46.4**	42.2	38.2	31.4
Cu-1-30-ZSM-5	2.4	30	8.0	9.7	41.3	63.4	72.8	**76.1**	71.9	65.2	62.4	58.4	53.4
Cu-1-55-ZSM-5	2.6	55	6.6	6.6	14.3	54.0	71.8	78.9	**79.0**	73.1	69.1	65.8	59.8
Cu-1-80-ZSM-5	4.4	80	1.0	4.0	22.4	63.2	66.4	**73.9**	73.4	67.5	59.1	59.0	58.1
Cu-2-30-ZSM-5	2.9	30	9.8	11.5	17.3	56.9	**75.0**	72.8	70.6	66.3	61.9	58.5	53.5
Cu-2-55-ZSM-5	3.7	55	13.0	15.0	25.6	62.3	**78.5**	75.4	74.2	68.9	65.0	58.1	54.0
Cu-2-80-ZSM-5	14.3	80	19.9	20.2	61.5	72.5	**77.6**	76.8	73.7	69.4	64.8	63.4	56.5

[a] W_{Cu}: percentage of Cu in the catalyst.
[b] T_u: ion exchange temperature.
[c] T_R: reaction temperature.

creased at higher contents. It is well known that Cu^{2+} ions have an important role in the selective catalytic reduction of NO_X with hydrocarbons [39]. In presence of propene, Cu^{2+} is reduced to Cu^+, and then Cu^+ would be oxidised back to Cu^{2+} by NO_X, thus completing the catalytic cycle [32,40]. Some authors have reported that the low coordination of the Cu^{2+} cations made them much more susceptible to redox chemistry when exposed to NO than a more highly coordinated Cu^{2+} cations [32,40,41].

In the case of ZSM-5-based catalyst, Cu^{2+} cations with high coordination would occupy the hidden positions in the framework of the zeolite, whereas the low coordinated cations would be located in more accessible positions for the reactant molecules. According to Bulanek et al. [28], Cu^{2+} ions presents in MFI, FER and MOR structures can be found forming one of the two most populated Cu ions types, denoted as the Cu-II and Cu-IV type ions [42]. The Cu-II type of ions exhibited pyramid coordination and high positive charge and are balanced by two species AlO_2^- of the zeolitic framework. The Cu-IV type of ions were ascribed to the Cu ions with close-up to planar coordination and a low positive charge, and are adjacent to single AlO_2^- anions. At low copper contents and a high concentration of aluminium the Cu-II type of ions prevails, whereas at high copper contents and a low concentration of aluminium in the framework the Cu-IV type of ions became predominant. The latter, although have lower coordination, exhibits an accessibility and reducibility higher than the former. Thus, Cu-IV should be the active sites for NO_X reduction to N_2. As expected, when the content of these species is higher, an increase of the catalytic activity is observed.

An increase of the ion exchange temperature leads to an increase of the metal contents in the catalysts and, therefore, to an increase of the Cu^{2+} content. As a consequence a light increase of the NO_X conversion is observed. However, when a second ion exchange step is carried out, a decrease of NO_X conversion to N_2 occurs, especially for mordenite-based catalysts. As abovementioned, an increase in Cu loading resulted in an increase in CuO aggregates. According to Bulanek et al. [28] the presence of CuO species resulted in a substantial increase of both the hydrocarbon conversion and selectivity to CO_2. The combustion of propene reduces its disponibility for the SCR of NO_X.

3.2. Co-zeolite-based catalysts

Similar to copper catalysts, sodium content decreases with the increase of the cobalt content (Table 1). Likewise, the same trends, as far as the effect of the type of zeolite, number of ion exchange steps and ion exchange temperature on the metal contents are concerned, observed with Cu-zeolite-based catalysts can be extrapolated to the Co-zeolite-based ones.

In the TPD analysis of Co-ZSM-5-based catalysts, a peak close to 300 °C associated to the presence of sodium cations was detected. Strong acidity was really meaningful in sam-

ples ion exchanged at 80 °C (with the highest Co content). Co-mordenite-based catalysts showed strong acidity as compared to Co-ZSM-5, due to the higher density of acid sites for the former zeolite. Nevertheless, an acidity decrease was observed with increasing the ion exchange temperature, due probably to the formation of big cobalt oxide particles, which could partially block the channels of the zeolite.

Fig. 3 shows the TPR profiles of the catalysts prepared with different Co contents. In all cases, two peaks are observed: one, in the range of 350–400 °C, corresponding to the reduction of Co_3O_4 cobalt oxide particles [43] and another one, close to 700 °C, corresponding to the reduction of Co^{2+} [44]. Several authors suggest that both species could be catalytically actives [43]. Cobalt oxide would firstly oxide NO to NO_2 that later could be quimisorbed as NO_y ($y \geq 2$) over the more actives Co^{2+} centers, where would be reduced to N_2 [43,45,46]. Some authors have even reported that only with the presence of isolated cobalt ions over Co-ZSM-5-based catalysts the NO_2 formation would not be favoured [44].

Small peaks observed in all TPR curves at lower temperatures are not due to a consumption of H_2, but the desorption of argon that it is hold in the channels of the zeolite [47].

Table 3 shows, for all the Co-zeolite-based catalysts, the total H_2 consumption (mol H_2/mol Co present in the catalyst) for the TPR experiments. According to earlier studies [43], the following reduction reaction can be assumed:

$$Co^{2+} + H_2 \rightarrow Co^0 + 2H^+$$

In the case of a complete reduction of all the Co^{2+} ions present over the catalysts, the molar ratio H_2/Co should be equal to 1. In ZSM-5-based catalysts, values lower to 1 were observed, except Co-2-80-ZSM-5. This fact would indicate that Co^{2+} ions would not have been reduced. These ions could be located in inaccessible sites [48] or could be forming part of the species with Co–Co bonds [43]. On the other hand, mordenite-based catalysts with higher metal content showed values of H_2 consumption higher than 1. This fact could be attributed to that part of the cobalt present in the samples would be as Co^{3+} species [43].

Table 3
Consumption of H_2 (mol H_2/mol Co present in the catalyst)

Catalyst	Cobalt content (wt.%)	H_2/Co (mol/mol)
Na-MOR	–	–
Co-1-30-MOR	3.0	1.115
Co-1-55-MOR	3.1	1.187
Co-1-80-MOR	3.2	1.424
Co-2-30-MOR	3.8	1.249
Co-2-55-MOR	4.0	1.316
Co-2-80-MOR	5.0	1.542
Na-ZSM-5	–	–
Co-1-30-ZSM-5	0.5	0.912
Co-1-55-ZSM-5	0.9	0.932
Co-1-80-ZSM-5	2.2	0.927
Co-2-30-ZSM-5	0.8	0.962
Co-2-55-ZSM-5	1.6	0.980
Co-2-80-ZSM-5	3.1	1.099

3.2.1. Catalytic activity

It is important to mention that cobalt is, along with copper, one of the most used metals to be supported for the selective catalytic reduction of nitrogen oxides [49]. Table 4 shows for all Co-zeolite-based catalysts, the NO_X conversion to N_2.

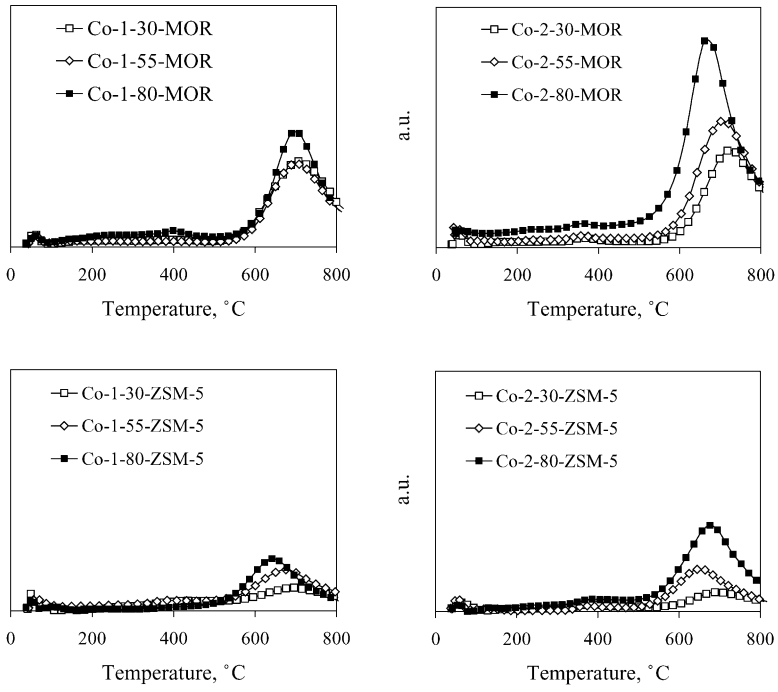

Fig. 3. TPR profile of the cobalt mordenite-based catalysts.

Table 4
NO_X conversion of NO to N_2 for the cobalt-based catalysts (no N_2O detected)

Catalyst	W_{Co} (wt.%)[a]	T_u (°C)[b]	NO_X conversion to N_2 (%)									
			T_R[c] = 200 °C	T_R = 250 °C	T_R = 300 °C	T_R = 325 °C	T_R = 350 °C	T_R = 375 °C	T_R = 400 °C	T_R = 425 °C	T_R = 450 °C	T_R = 475 °C	T_R = 500 °C
Co-1-30-MOR	3.0	30	8.9	12.2	21.6	35.1	65.1	77.7	**79.9**	78.0	73.3	68.7	60.1
Co-1-55-MOR	3.1	55	14.7	16.0	19.2	31.1	57.6	81.4	**82.0**	78.1	73.9	67.2	58.7
Co-1-80-MOR	3.2	80	25.2	25.1	26.8	56.5	70.0	80.6	**84.8**	77.5	73.3	71.2	64.0
Co-2-30-MOR	3.8	30	16.8	19.4	24.8	39.8	47.8	49.1	**52.8**	50.8	45.3	41.2	34.8
Co-2-55-MOR	4.0	55	2.8	4.3	14.8	17.2	36.7	53.3	**60.9**	53.8	49.1	45.2	29.1
Co-2-80-MOR	5.0	80	9.4	11.5	14.5	27.2	41.8	**54.3**	53.1	48.9	38.6	32.3	25.2
Co-1-30-ZSM-5	0.5	30	19.9	20.5	21.6	21.6	31.3	53.2	**62.2**	56.3	54.3	52.5	52.4
Co-1-55-ZSM-5	0.9	55	26.1	22.5	26.3	35.0	51.8	**66.8**	62.2	53.5	48.6	40.9	37.0
Co-1-80-ZSM-5	2.2	80	12.5	14.4	17.3	31.3	38.5	58.9	**69.6**	55.6	53.7	47.4	39.5
Co-2-30-ZSM-5	0.8	30	12.8	13.4	13.1	18.2	20.9	44.4	**63.9**	56.0	54.1	49.1	43.0
Co-2-55-ZSM-5	1.6	55	7.0	7.0	12.0	29.3	43.3	**61.2**	61.0	50.8	48.3	39.6	33.8
Co-2-80-ZSM-5	3.1	80	12.0	13.8	14.9	22.3	42.1	54.1	**58.4**	54.3	52.0	49.9	33.5

[a] W_{Co}: percentage of Co in the catalyst.
[b] T_u: ion exchange temperature.
[c] T_R: reaction temperature.

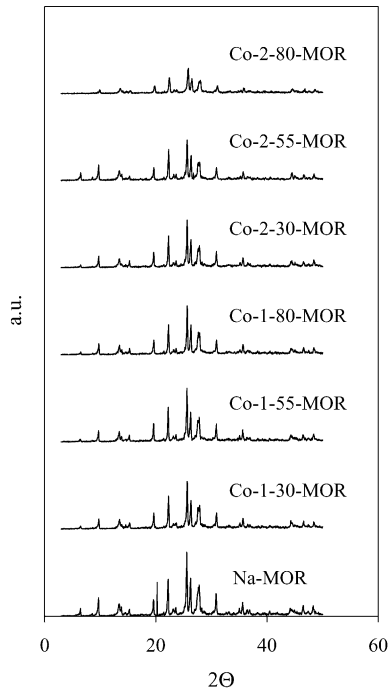

Fig. 4. XRD spectra of cobalt-based catalysts.

For all the samples, temperature corresponding to the maximum NO_X conversion was close to 400 °C. Similar trend has been observed by Lukyanov et al. [50] using CoZSM-5 as the catalyst and methane as the hydrocarbon.

The best catalytic results were reached for the catalysts ion exchanged once. The second ion exchange step results in an increase of the metal content that favours the formation of oxide particles that do not promote the SCR of NO_X reaction. Furthermore, the incorporation of a big amount of cobalt would allow cobalt atoms to link with six oxygen atoms of the zeolitic framework, causing its deformation and, this way, an average crystallinity loss of 35% (Fig. 4). This effect has also been observed in ferrierite zeolites [48].

Precisely, the most active catalysts reported in this paper (Co-1-30-MOR, Co-1-55-MOR and Co-1-80-MOR) are Co-based catalyst. This finding is in good agreement with those reported by other authors [44,51]. Li and Armor [52] observed that only with some types of zeolites, cobalt cations find a suitable electronic environment to be effective in the SCR of NO_X using methane as the reductant. Generally, cobalt exchanged zeolites have a better catalytic behaviour than copper exchanged ones, due to the higher stability of the divalent state [48].

3.3. Ni-zeolite-based catalysts

All the Ni-zeolite-based catalysts showed a lower ion exchange level than that observed with Cu and Co ion exchanged samples (Table 1).

Fig. 5 shows TPR profiles for the Ni-zeolite-based catalysts. At low metal contents, a peak close to 505 °C, corre-

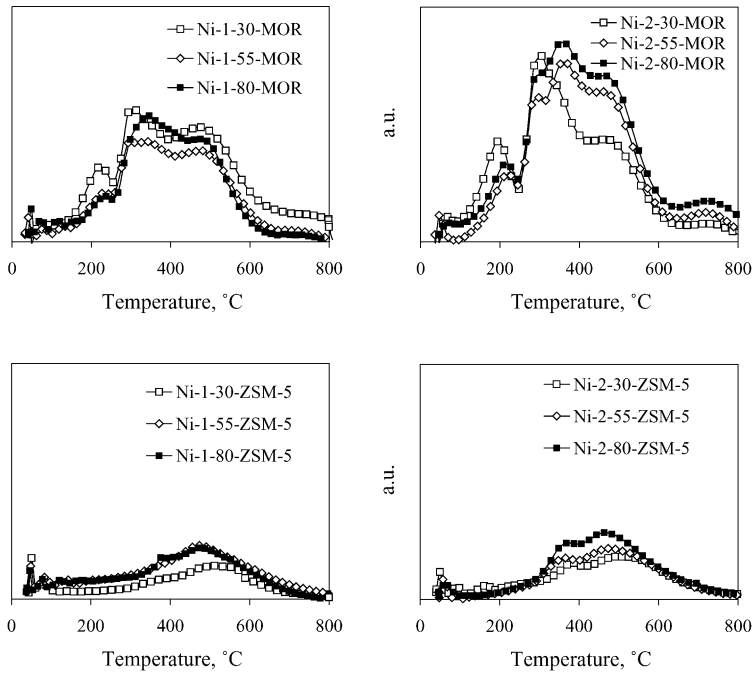

Fig. 5. TPR profile of the nickel mordenite-based catalysts.

sponding to the reduction of Ni^{2+}, is observed [53]. This peak shifts towards lower temperatures (470–490 °C) as the metal content increases. Besides this peak, two additional peaks appear at 270 and 380 °C, whose intensity increases with the metal content. These peaks would correspond to the reduction of nickel oxide which weakly interacts with the support.

3.3.1. Catalytic activity

Table 5 shows, for all the Ni-zeolite-based catalysts, the NO_X conversion to N_2. Due to the low metal contents, all the ZSM-5-based catalysts show a similar catalytic behaviour. According to Table 1 the ion exchange degree for these samples is below 100%.

In both sets of catalysts, the maximum of NO_X conversion decreases with increasing both ion exchange temperature and number of ion exchange steps. It is remarkable the activity of the sample Ni-1-30-MOR that is higher than any of the Cu-zeolite-based catalysts and slightly lower than the best Co-zeolite-based catalyst (Co-1-80-MOR).

3.4. Mn-zeolite-based catalysts

The manganese content increases with the number ion exchange of steps and ion exchange temperature (Table 1). In all cases, the ion exchange level is lower than 100%. As expected, mordenite-based catalysts presented higher metal content than ZSM-5.

For Mn-ZSM-5-based catalysts, only a peak centered at 300 °C and related to the presence of sodium cations, appears in the TPD analysis. As a consequence of the replacement of sodium ions by manganese ones, a decrease of both weak and total acidity is observed, being the values of strong acidity for Mn-zeolite very low.

In the case of Mn-mordenite-based catalysts, an increase of the metal content produces a loss of weak acidity. In this case, higher metal contents lead to a light increase of the strong acidity of the catalyst.

Fig. 6 shows TPR profiles for all Mn-zeolite-based catalysts. Two peaks centered at 400 °C and in the range 600–620 °C were observed. The first peak corresponds to the reduction of MnO_2 to MnO over the formation of Mn_2O_3 and Mn_3O_4 as intermediary [54]. The peak centered at 600–620 °C corresponds to the reduction of Mn^{3+} (as $Mn^{3+}(O^-)$), to Mn^{2+} [55,56]. According to Bell et al. [56], the active specie for the SCR reaction would be the Mn^{3+} ion. This specie would be reduced by the hydrocarbon to Mn^{2+}; consecutively, Mn^{2+} would be oxidised back to Mn^{3+} by NO_X.

3.4.1. Catalytic activity

Table 6 shows for all Mn-zeolite-based catalysts, the NO_X conversion to N_2. Mn-ZSM-5-based catalysts showed the maximum of NO_X conversion at 425 °C, whereas Mn-mordenite-based catalysts showed it at 400–450 °C. The catalytic results obtained with the Mn-zeolite-based catalysts were worse compared to those obtained with Cu, Co or Ni-zeolite-based ones.

3.5. TOF of all the catalysts at 400 °C

Fig. 7 shows for a temperature of 400 °C the values of the velocity of consumption of NO per mol of metal as

Table 5
NO_X conversion of NO to N_2 for the nickel-based catalysts (no N_2O detected)

Catalyst	W_{Ni} (wt.%)[a]	T_u (°C)[b]	NO_X conversion to N_2 (%)										
			T_R[c] = 200 °C	T_R = 250 °C	T_R = 300 °C	T_R = 325 °C	T_R = 350 °C	T_R = 375 °C	T_R = 400 °C	T_R = 425 °C	T_R = 450 °C	T_R = 475 °C	T_R = 500 °C
Ni-1-30-MOR	2.4	30	8.5	6.4	4.3	10.6	14.9	27.3	37.0	59.5	**79.8**	72.0	62.2
Ni-1-55-MOR	2.5	55	4.9	21.4	23.3	22.9	23.9	35.7	59.1	**75.4**	69.9	61.9	41.8
Ni-1-80-MOR	2.7	80	18.9	20.6	28.3	29.7	32.7	40.1	56.7	**71.2**	66.4	59.8	53.1
Ni-2-30-MOR	3.0	30	14.6	15.6	18.8	18.8	30.7	43.8	64.6	**67.9**	61.7	58.5	47.8
Ni-2-55-MOR	3.2	55	11.6	13.6	23.0	26.5	30.6	36.1	49.5	**60.2**	52.9	46.3	45.6
Ni-2-80-MOR	3.3	80	9.3	12.4	15.5	18.8	26.9	39.2	**44.6**	42.4	40.0	33.5	32.3
Ni-1-30-ZSM-5	0.3	30	16.7	12.1	12.1	12.6	16.6	32.6	68.4	**76.6**	70.4	64.3	59.5
Ni-1-55-ZSM-5	0.6	55	12.0	9.3	8.8	10.1	14.3	27.9	71.3	**74.9**	67.6	63.6	58.6
Ni-1-80-ZSM-5	0.8	80	10.2	10.2	13.3	14.3	25.2	45.9	**74.6**	72.8	65.7	63.4	61.9
Ni-2-30-ZSM-5	0.5	30	9.6	8.5	10.6	14.9	19.1	33.6	**69.7**	69.1	64.3	60.4	56.8
Ni-2-55-ZSM-5	0.7	55	17.4	10.7	12.6	13.6	21.7	35.7	**72.8**	68.3	63.1	60.3	43.2
Ni-2-80-ZSM-5	1.1	80	14.9	12.5	15.8	18.8	24.4	41.6	**72.1**	68.6	64.4	59.6	53.3

[a] W_{Ni}: percentage of Co in the catalyst.
[b] T_u: ion exchange temperature.
[c] T_R: reaction temperature.

Table 6
NO_X conversion of NO to N_2 for the manganese-based catalysts (no N_2O detected)

Catalyst	W_{Mn} (wt.%)[a]	T_u (°C)[b]	NO_X conversion to N_2 (%)										
			T_R[c] = 200 °C	T_R = 250 °C	T_R = 300 °C	T_R = 325 °C	T_R = 350 °C	T_R = 375 °C	T_R = 400 °C	T_R = 425 °C	T_R = 450 °C	T_R = 475 °C	T_R = 500 °C
Mn-1-30-MOR	1.8	30	17.8	18.9	23.2	24.2	35.4	44.0	50.2	51.2	**53.2**	51.3	49.2
Mn-1-55-MOR	2.2	55	130	11.4	14.0	20.9	30.3	45.1	50.5	60.0	**61.4**	56.6	57.0
Mn-1-80-MOR	2.8	80	14.7	14.1	25.8	32.9	39.9	53.5	56.9	**60.0**	59.3	58.7	54.0
Mn-2-30-MOR	3.0	30	18.9	14.7	21.5	28.4	44.0	64.4	**73.6**	71.5	66.9	62.6	54.6
Mn-2-55-MOR	3.2	55	13.4	9.2	19.0	26.1	35.2	41.5	**55.9**	53.8	50.7	46.5	40.8
Mn-2-80-MOR	3.7	80	13.4	16.5	19.8	34.6	42.8	45.8	48.4	**50.4**	47.4	43.9	37.2
Mn-1-30-ZSM-5	0.3	30	10.9	12.0	16.3	17.4	26.1	44.0	49.5	**52.7**	49.5	44.7	40.8
Mn-1-55-ZSM-5	0.7	55	14.6	14.6	14.2	17.0	23.4	34.5	46.3	**54.6**	49.9	44.4	41.9
Mn-1-80-ZSM-5	1.2	80	12.8	14.2	15.8	16.1	20.8	29.7	46.8	**65.2**	63.8	57.5	49.2
Mn-2-30-ZSM-5	0.7	30	16.2	16.8	22.5	33.3	35.4	37.1	42.6	**43.6**	43.0	38.2	34.7
Mn-2-55-ZSM-5	1.0	55	11.3	12.0	12.0	17.0	23.1	33.3	45.0	49.9	**52.3**	48.0	45.4
Mn-2-80-ZSM-5	1.8	80	15.4	17.0	19.1	24.1	32.7	44.9	50.9	**54.3**	51.1	47.0	44.6

[a] W_{Mn}: percentage of Mn in the catalyst.
[b] T_u: ion exchange temperature.
[c] T_R: reaction temperature.

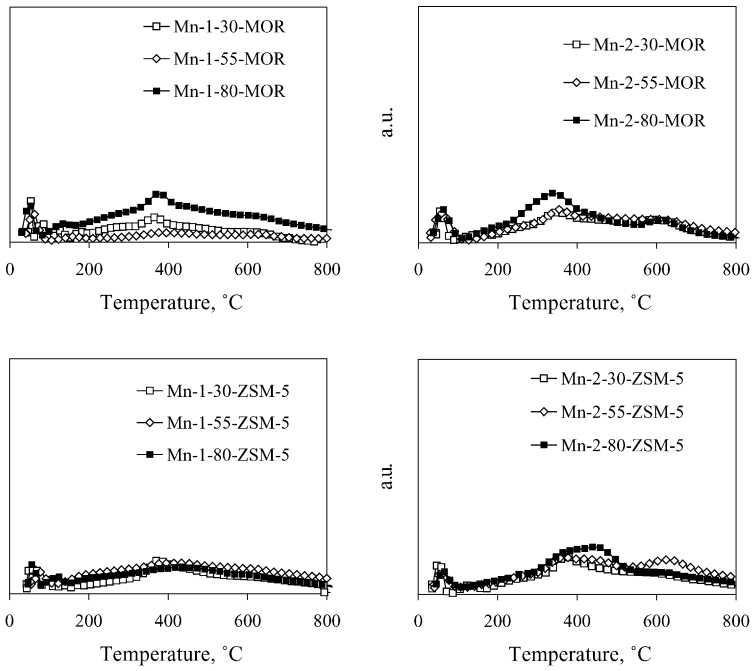

Fig. 6. TPR profile of the manganese mordenite-based catalysts.

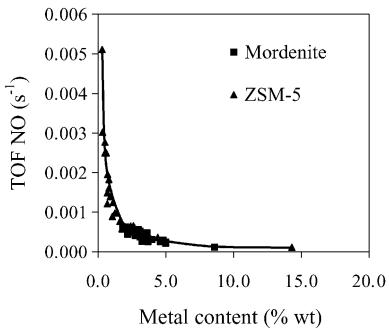

Fig. 7. TOF of all the catalysts. Conditions: NO = 1000 ppm; C_3H_6 = 1000 ppm; O_2 = 5%; He = balance. Flow = 125 ml/min GHSV = 15,000 h^{-1}. Reaction temperature = 400 °C.

a function of the metal content. It has been supposed that all the metal is active for the reaction. NO TOF decreases abruptly with the metal content until a value of 5.0%. It is remarkable that, regardless the type of zeolite and ion exchanged metal introduced in the catalysts, all the experimental points are well correlated by a unique curve. This fact would indicate that the controlling step of the SCR reaction with all these catalysts would be the chemical reaction and that the catalytically active metal species must have a similar behaviour. Similar trends were observed at 375, 425 and 450 °C.

4. Conclusions

Selective catalytic reduction of NO by propene was investigated on Cu, Co, Ni and Mn ion-exchanged ZSM-5 and mordenite in the presence of excess of oxygen. H_2-TPR results showed that for copper catalysts metal was mainly present in the form of isolated Cu^{2+} strongly coordinated to the framework oxygen atoms of the zeolite. Cobalt, nickel and manganese were present in the form Co^{2+} and Co^{3+}, Ni^{2+}, Mn^{3+} and Mn^{4+}, respectively.

The catalytic activity showed for all the catalysts increased with increasing metal content reaching a maximum of NO_X conversion, and then decreased at higher contents. In turn, NO_X conversion increased with the reaction temperature passing through a maximum, and then decreased at higher temperatures, due to the combustion of the hydrocarbon, which reduced the amount of reductant and became dominant at higher temperatures. The maximum was located in the range 350–425 °C.

NO TOF for all the catalysts here prepared was analyzed at 375–425 °C. It was observed that this parameter decreased abruptly with the metal content and, regardless, the type of zeolite and ion exchanged metal introduced in the catalysts, all the experimental points were well correlated by a unique curve. This fact would indicate that the controlling step of the SCR reaction with all these catalysts would be the chemical reaction and that the catalytic active species must have a similar behaviour.

Acknowledgments

Financial support from both the European Commission (Contract ERK5-CT-1999-00001) and the Ministerio de Ciencia y Tecnología (CICYT) of Spain (Project PPQ2001-1195-C02-01) are gratefully acknowledged.

References

[1] C.N. Costa, T. Anastasiadou, A.M. Efstathiou, J. Catal. 194 (2000) 250.
[2] M. Shelef, Chem. Rev. 95 (1995) 209.
[3] M. Iwamoto, Catal. Today 29 (1996) 29.
[4] A.W. Aylor, S.C. Larsen, J.A. Reimer, A.T. Bell, J. Catal. 157 (1995) 592.
[5] Y. Li, J.N. Armor, Appl. Catal. B 5 (1995) 257.
[6] B.J. Adelman, T. Beutel, G.-D. Lei, W.M.H. Sachtler, J. Catal. 158 (1996) 327.
[7] K.A. Bethke, H.H. Kung, J. Catal. 172 (1997) 93.
[8] R. Burch, A.A. Shestov, J.A. Sullivan, J. Catal. 182 (1999) 497.
[9] Y.-H. Chin, A. Pisanu, L. Serventi, W.E. Alvarez, D.E. Resasco, Catal. Today 54 (1999) 419.
[10] D.K. Captain, M.D. Amiridis, J. Catal. 184 (1999) 377.
[11] S. Xie, M.P. Rosynek, J.H. Lunsford, J. Catal. 188 (1999) 24.
[12] F.C. Meunier, J.P. Breen, V. Zuzaniuk, M. Olsson, J.R.H. Ross, J. Catal. 187 (1999) 493.
[13] K. Shimizu, F. Okada, Y. Nakamura, A. Satsuma, T. Hattori, J. Catal. 195 (2000) 151.
[14] R.T. Yang, N. Tharappiwattananon, R.Q. Long, Catal. Appl. B 19 (1998) 289.
[15] M. Iwamoto, H. Furukawa, Y. Mine, F. Uemura, S. Mikuriya, S. Kagawa, J. Chem. Soc., Chem. Commun. 16 (1986) 1272.
[16] M.D. Amiridis, T. Zhang, R.J. Farrauto, Appl. Catal. B 10 (1996) 203.
[17] M. Shelef, Catal. Lett. 15 (1992) 305.
[18] C. Yokoyama, M. Misono, J. Catal. 150 (1994) 9.
[19] K. Shimizu, H. Kawabata, H. Maeshima, A. Satsuma, T. Hattori, J. Phys. Chem. B 104 (2000) 2885.
[20] K. Shimizu, H. Maeshima, H. Yoshida, A. Satsuma, T. Hattori, Phys. Chem. Chem. Phys. 2 (2000) 2435.
[21] J.L. Valverde, A. De Lucas, P. Sanchez, F. Dorado, A. Romero, Appl. Catal. B 43 (2003) 43.
[22] J.L. Valverde, A. De Lucas, P. Sanchez, F. Dorado, A. Romero, Stud. Surf. Sci. Catal. A 142 (2002) 723.
[23] J.L. Valverde, A. De Lucas, F. Dorado, R. Sun-Kou, P. Sanchez, I. Asencio, A. Garrido, A. Romero, Ind. Eng. Chem. Res. 42 (2003) 2783.
[24] J.L. Valverde, F. Dorado, P. Sanchez, I. Asencio, A. Romero, Ind. Eng. Chem. Res. 42 (2003) 3871.
[25] I. Asencio, F. Dorado, J.L. Valverde, A. De Lucas, P. Sanchez, Stud. Surf. Sci. Catal. A 142 (2002) 731.
[26] J.L. Valverde, F. Dorado, P. Sanchez, I. Asencio, A. Romero, Interfacial Applications of Environmental Engineering, Marcel Dekker Inc., New York, 2003.
[27] C. Torre-Abreu, M.F. Ribeiro, C. Henriques, F.R. Ribeiro, Appl. Catal. B 13 (1997) 251.
[28] R. Bulanek, B. Wichterlova, Z. Sobalik, J. Tichy, Appl. Catal. B 31 (2001) 13.
[29] E. Costa, M.A. Uguina, A. De Lucas, J. Blanes, J. Catal. 107 (1987) 317.
[30] M.A. Uguina, A. De Lucas, F. Ruiz, D.P. Serrano, Ind. Eng. Chem. Res. 34 (1995) 451.
[31] W.M.H. Sachtler, Z. Zhang, Adv. Catal. 39 (1993) 129.
[32] G. Delahay, B. Coq, L. Broussous, Appl. Catal. B 12 (1997) 49.
[33] S. Tanabe, H. Matsumoto, Appl. Catal. 45 (1988) 27.
[34] J.A. Sullivan, J. Cunningham, Appl. Catal. B 15 (1998) 275.
[35] J. Sarkany, J.L. D'Itri, W.M.H. Sachtler, Catal. Lett. 16 (1992) 241.
[36] W. Li, M. Sirilumpen, R.T. Yang, Appl. Catal. B 11 (1997) 347.
[37] M. Iwamoto, N. Mizuno, H. Yahiro, Stud. Surf. Sci. Catal. 75 (1993) 1285.
[38] A. Corma, V. Fornes, E. Palomares, Appl. Catal. B 11 (1997) 233.
[39] M. Shimokawabe, K. Tadokoro, S. Sasaki, N. Takezawa, Appl. Catal. A 166 (1998) 215.
[40] R.Q. Long, R.T. Yang, Ind. Eng. Chem. Res. 38 (1999) 873.
[41] M.P. Attfield, S.J. Weigel, A.K. Cheetham, J. Catal. 170 (1997) 227.
[42] J. Dedecek, Z. Sobalik, Z. Tvaruazkova, D. Kaucky, B. Wichterlova, J. Phys. Chem. 99 (1995) 16327.
[43] X. Wang, H.-Y. Chen, W.M.H. Sachtler, Appl. Catal. B 26 (2000) 227.
[44] A.Yu. Stakheev, C.W. Lee, S.J. Park, P.J. Chong, Catal. Lett. 38 (1996) 271.
[45] C. De Correa, A.P. de Luz Villa de, Catal. Lett. 53 (1998) 205.
[46] A. Shichi, A. Satsuma, T. Hattori, Chem. Lett. (2001) 44.
[47] D.L. Hoang, H. Berndt, H. Miessner, E. Schreier, J. Voelter, H. Lieske, Appl. Catal. A 114 (1994) 295.
[48] Z. Sobalik, J. Dedecek, I. Ikonnikov, B. Wichterlova, Micropor. Mesopor. Mater. 21 (1998) 525.
[49] H. Hamada, Y. Kintaichi, M. Sasaki, T. Ito, M. Tabata, Appl. Catal. 75 (1991) 1.
[50] D.B. Lukyanov, E.A. Lombardo, G.A. Sill, J.L. d'Itri, W.K. Hall, J. Catal. 163 (1996) 447.
[51] A.-Z. Ma, M. Muhler, W. Grunert, Appl. Catal. B 27 (2000) 37.
[52] Y. Li, J.N. Armor, J. Catal. 150 (1994) 376.
[53] P. Canizares, A. De Lucas, F. Dorado, A. Duran, I. Asencio, Appl. Catal. A 169 (1998) 137.
[54] M. Richter, H. Kosslick, R. Fricke, Stud. Surf. Sci. Catal. B 130 (2000) 1517.
[55] R. Mariscal, M.A. Pena, J.L.G. Fierro, Appl. Catal. A 131 (1995) 243.
[56] A.T. Bell, L.J. Lobree, A.W. Aylor, J.A. Reimer, Proceedings of the 214th ACS National Meeting, Las Vegas, NV, September 7–11, 1997, p. 815.